J. Plasma Physics (2010), *vol.* 76, *part* 1, *pp.* 7–17.
doi:10.1017/S0022377809990316

Letter to the Editor

Dispersion properties of electrostatic oscillations in quantum plasmas

BENGT ELIASSON[1,2] and PADMA KANT SHUKLA[1]

[1] Institut für Theoretische Physik IV, Ruhr-Universität Bochum, D-44780 Bochum, Germany
(bengt@tp4.ruhr-uni-bochum.de)
[2] Department of Physics, Umeå University, SE-901 87 Umeå, Sweden

(Received 10 September 2009 and accepted 22 September 2009, first published online 27 October 2009)

Abstract. We present a derivation of the dispersion relation for electrostatic oscillations in a zero-temperature quantum plasma, in which degenerate electrons are governed by the Wigner equation, while non-degenerate ions follow the classical fluid equations. The Poisson equation determines the electrostatic wave potential. We consider parameters ranging from semiconductor plasmas to metallic plasmas and electron densities of compressed matter such as in laser compression schemes and dense astrophysical objects. Owing to the wave diffraction caused by overlapping electron wave function because of the Heisenberg uncertainty principle in dense plasmas, we have the possibility of Landau damping of the high-frequency electron plasma oscillations at large enough wavenumbers. The exact dispersion relations for the electron plasma oscillations are solved numerically and compared with the ones obtained by using approximate formulas for the electron susceptibility in the high- and low-frequency cases.

1. Introduction

The field of quantum plasma physics is becoming of increasing current interest (Bonitz et al. 2003; Manfredi 2005; Shukla 2006, 2009; Shaikh 2007; Crouseilles 2008; Serbeto 2008), motivated by its potential applications in modern technology (e.g. metallic and semiconductor nanostructures including metallic nanoparticles, metal clusters, thin metal films, spintronics, nanotubes, quantum well and quantum dots, nano-plasmonic devices, quantum X-ray free-electron lasers and the like). In dense quantum plasmas and in the Fermi gas of metals, the number densities of degenerate electrons are extremely high so that their wave functions overlap, and the electrons therefore obey the Fermi–Dirac statistics. The collective oscillations in quantum plasmas have been studied by several authors in the past (Bohm 1952; Klimontovich and Silin 1952; Bohm and Pines 1953; Ferrel 1957; Klimontovich and Silin 1961; Pines 1961) with applications to the Fermi plasmas in metals and semiconductors and to electrostatic oscillations in quantum pair plasmas (Mendonça et al. 2008). Watanabe (1956) studied experimentally the Bohm–Pines dispersion relation of the electron plasma oscillations by measuring the energy

loss of electrons by the excitation of collective modes in metals. The Fermi degenerate dense plasma may also arise when a pellet of hydrogen is compressed to many times the solid density in the fast-ignition scenario for inertial confinement fusion (Azechi et al. 1991, 2006; Son and Fisch 2005; Lindl 1995; Tabak et al. 1994, 2005). Since there has been an impressive development in the field of short pulse petawatt laser technology, it is highly likely that such plasma conditions can be achieved by intense laser pulse compression using powerful X-ray pulses. Here ultrafast X-ray Thomson scattering techniques can be used to measure the features of laser-enhanced plasma lines, which will, in turn, give invaluable information regarding the equation of state of shock-compressed dense matters. Recently, spectrally resolved X-ray scattering measurements (Kritcher et al. 2008; Lee et al. 2009) have been performed in dense plasmas, allowing accurate measurements of the electron velocity distribution function, temperature and ionization state and of plasmons in the warm dense matter regime (Glenzer et al. 2007). This novel technique promises to access the degenerate, the closely coupled and the ideal plasma regime, making it possible to investigate extremely dense states of matter, such as the inertial confinement fusion fuel during compression, reaching super-solid densities.

In this paper, we present a study of the dispersion properties of electrostatic oscillations in a dense quantum plasma, by employing the Wigner–Poisson model. We point out the differences between different regimes comprising the relatively low-density regime of semiconductor plasmas and the higher-density regimes corresponding to metallic electron densities and laser-compressed plasmas, as well as plasmas in dense astrophysical objects such as white dwarf stars.

2. Derivation of the dispersion relation for the Wigner–Poisson system

We here present a derivation of the dispersion relation for electrostatic waves in a degenerate quantum plasma. The electron dynamics is governed by the Wigner equation

$$\frac{\partial f_1}{\partial t} + \mathbf{v}\cdot\nabla f_1 = -\frac{iem_{\rm e}^3}{(2\pi)^3\hbar^4}\int\int d^3\lambda d^3v' \exp\left[i\frac{m_{\rm e}}{\hbar}(\mathbf{v}-\mathbf{v}')\cdot\boldsymbol{\lambda}\right] \times\left[\phi_1\left(\mathbf{x}+\frac{\boldsymbol{\lambda}}{2},t\right)-\phi_1\left(\mathbf{x}-\frac{\boldsymbol{\lambda}}{2},t\right)\right] f_0(\mathbf{v}'), \tag{2.1}$$

where the electrostatic potential ϕ is given by the Poisson equation

$$\nabla^2\phi_1 = \frac{e}{\epsilon_0}\left(\int f_1 d^3v - n_{i1}\right). \tag{2.2}$$

Here e is the magnitude of the electron charge; $m_{\rm e}$ is the electron mass; $\hbar$ is the Planck constant divided by 2π; and ϵ_0 is the permittivity of free space. Furthermore, f_0 and n_0 denote the equilibrium electron distribution function and the electron number density, respectively, while f_1, ϕ_1 and n_{i1} denote the perturbed electron distribution function, the electrostatic potential and the ion number density, respectively.

Assuming that f_1, ϕ_1 and n_{i1} are proportional to $\exp(-i\omega t + i\boldsymbol{k}\cdot\mathbf{x})$, where ω is the frequency and $\boldsymbol{k}$ is the wave vector, we respectively obtain the following from

https://doi.org/10.1017/S0022377809990316 Published online by Cambridge University Press

(2.1) and (2.2):

$$(\omega - \boldsymbol{k}\cdot\mathbf{v})f_1 = \frac{em_{\mathrm{e}}^3}{(2\pi)^3\hbar^4}\int\int d^3\lambda d^3v' \exp\left[i\frac{m_{\mathrm{e}}}{\hbar}(\mathbf{v}-\mathbf{v}')\cdot\boldsymbol{\lambda}\right] \times \left[e^{i\boldsymbol{k}\cdot\boldsymbol{\lambda}/2} - e^{-i\boldsymbol{k}\cdot\boldsymbol{\lambda}/2}\right] f_0(\mathbf{v}')\phi_1(\omega,\boldsymbol{k}), \tag{2.3}$$

$$k^2\phi_1 = -\frac{e}{\epsilon_0}\left(\int f_1 d^3v - n_{i1}\right). \tag{2.4}$$

Since ions are non-degenerate in quantum plasmas, for $\omega \gg kV_{Ti}$ we have

$$n_{i1} = -\frac{\epsilon_0 k^2}{e}\chi_i\phi, \tag{2.5}$$

where

$$\chi_i = -\frac{\omega_{\mathrm{pi}}^2}{\omega^2} \tag{2.6}$$

is the ion susceptibility; V_{Ti} is the ion thermal speed; and ω_{pi} is the ion plasma frequency.

Rewriting (2.3) as

$$(\omega - \boldsymbol{k}\cdot\mathbf{v})f_1 = \frac{iem_{\mathrm{e}}^3}{(2\pi)^3\hbar^4}\int\int d^3\lambda d^3v' \times \left\{\exp\left[\frac{m_{\mathrm{e}}}{\hbar}(\mathbf{v}-\mathbf{v}')\cdot\boldsymbol{\lambda} + i\boldsymbol{k}\cdot\boldsymbol{\lambda}/2\right] - \exp\left[i\frac{m_{\mathrm{e}}}{\hbar}(\mathbf{v}-\mathbf{v}')\cdot\boldsymbol{\lambda} - i\boldsymbol{k}\cdot\boldsymbol{\lambda}/2\right]\right\} f_0(\mathbf{v}')\phi_1(\omega,\boldsymbol{k}) \tag{2.7}$$

and performing the integration over $\boldsymbol{\lambda}$ space, we have

$$(\omega - \mathbf{v}\cdot\boldsymbol{k})f_1 = \frac{em_{\mathrm{e}}^3}{\hbar^4}\int d^3v' \left\{\delta\left[\frac{m_{\mathrm{e}}}{\hbar}(\mathbf{v}-\mathbf{v}') + \frac{\boldsymbol{k}}{2}\right] - \delta\left[\frac{m_{\mathrm{e}}}{\hbar}(\mathbf{v}-\mathbf{v}') - \frac{\boldsymbol{k}}{2}\right]\right\} f_0(\mathbf{v}')\phi_1(\omega,\boldsymbol{k}), \tag{2.8}$$

where δ is the Dirac delta function. Now, the integration can be performed over the $\mathbf{v}'$ space, obtaining the result

$$(\omega - \boldsymbol{k}\cdot\mathbf{v})f_1 = \frac{e}{\hbar}\left[f_0\left(\mathbf{v} + \frac{\hbar\boldsymbol{k}}{2m_{\mathrm{e}}}\right) - f_0\left(\mathbf{v} - \frac{\hbar\boldsymbol{k}}{2m_{\mathrm{e}}}\right)\right]\phi_1(\omega,\boldsymbol{k}). \tag{2.9}$$

Eliminating n_{i1} and f_1 in (2.4) with the help of (2.5) and (2.9), we obtain the dispersion relation

$$1 + \chi_{\mathrm{e}} + \chi_i = 0, \tag{2.10}$$

where the ion susceptibility is given by (2.6), and the electron susceptibility is given by

$$\chi_{\mathrm{e}} = -\frac{4\pi e^2k^2}{\hbar}\int\left[\frac{f_0\left(\mathbf{v} + \frac{\hbar\boldsymbol{k}}{2m_{\mathrm{e}}}\right)}{(-\omega + \boldsymbol{k}\cdot\mathbf{v})} - \frac{f_0\left(\mathbf{v} - \frac{\hbar\boldsymbol{k}}{2m_{\mathrm{e}}}\right)}{(-\omega + \boldsymbol{k}\cdot\mathbf{v})}\right] d^3u. \tag{2.11}$$

https://doi.org/10.1017/S0022377809990316 Published online by Cambridge University Press

Suitable changes of variables in the two terms in square brackets in (2.11) now give

$$\chi_{\rm e} = -\frac{4\pi e^2 k^2}{\hbar}\int\left[\frac{1}{[-\omega+\boldsymbol{k}\cdot(\mathbf{u}-\frac{\hbar\boldsymbol{k}}{2m_{\rm e}})]}-\frac{1}{[-\omega+\boldsymbol{k}\cdot(\mathbf{u}+\frac{\hbar\boldsymbol{k}}{2m_{\rm e}})]}\right]f_0(\mathbf{u})d^3u, \quad (2.12)$$

which can be rewritten as

$$\chi_{\rm e} = -\frac{4\pi e^2}{m_{\rm e}}\int\frac{f_0(\mathbf{u})}{(\omega-\boldsymbol{k}\cdot\mathbf{u})^2-\frac{\hbar^2k^4}{4m_{\rm e}^2}}d^3u. \quad (2.13)$$

This expression was also derived by Bohm and Pines (1953), using a series of canonical transformations of the Hamiltonian of the system (see for example the dispersion relation (57) in their paper), and by Ferrel (1957), using the method of self-consistent fields.

We now choose a coordinate system such that the x axis is aligned with the wave vector $\boldsymbol{k}$. Then, (2.13) takes the form

$$\chi_{\rm e} = -\frac{4\pi e^2}{m_{\rm e}}\int\frac{f_0(\mathbf{u})}{(\omega-ku_x)^2-\frac{\hbar^2k^4}{4m_{\rm e}^2}}d^3u. \quad (2.14)$$

We next consider a dense plasma with degenerate electrons in the zero-temperature limit. Then, the background distribution function takes the simple form

$$f_0 = \begin{cases} 2\left(\frac{m_{\rm e}}{2\pi\hbar}\right)^3, & |\mathbf{u}|\leqslant V_{\rm Fe},\\ 0, & \text{elsewhere,}\end{cases} \quad (2.15)$$

where $V_{\rm Fe} = (2\mathscr{E}_{\rm Fe}/m_{\rm e})^{1/2}$ is the speed of an electron on the Fermi surface and $\mathscr{E}_{\rm Fe} = (3\pi^2 n_0)^{2/3}\hbar^2/(2m_{\rm e})$ is the Fermi energy. The integration in (2.14) can be performed over velocity space perpendicular to u_x, using cylindrical coordinate in u_y and u_z, obtaining the result

$$\chi_{\rm e} = -\frac{4\pi e^2}{m_{\rm e}}\int\frac{F_0(u_x)}{(\omega-ku_x)^2-\frac{\hbar^2k^4}{4m_{\rm e}^2}}du_x, \quad (2.16)$$

where

$$F_0(u_x) = \int\int f_0(\mathbf{u})du_y du_z = 2\pi\int_0^{\sqrt{V_{\rm Fe}^2-u_x^2}} 2\left(\frac{m_{\rm e}}{2\pi\hbar}\right)^3 u_\perp\, du_\perp$$

$$= \begin{cases} 2\pi\left(\frac{m_{\rm e}}{2\pi\hbar}\right)^3(V_{\rm Fe}^2-u_x^2), & |u_x|\leqslant V_{\rm Fe},\\ 0, & \text{elsewhere.}\end{cases} \quad (2.17)$$

It is interesting to note that the distribution, which is flat topped in three dimensions, becomes parabola shaped in the remaining velocity dimension after the integration over the two perpendicular velocity dimensions. Hence, the electron distribution function $F_0(u_x)$ in (2.17) may support Landau damping if the pole of the denominator in (2.16) falls into the range of negative slope of $F_0(u_x)$ in velocity

https://doi.org/10.1017/S0022377809990316 Published online by Cambridge University Press

space. Equation (2.16) can be written as

$$\chi_{\rm e} = -\frac{8\pi^2 e^2}{m_{\rm e}} \left(\frac{m_{\rm e}}{2\pi\hbar}\right)^3 \int_{-V_{\rm Fe}}^{V_{V\,e}} \frac{V_{\rm Fe}^2 - u_x^2}{(\omega - ku_x)^2 - \frac{\hbar^2 k^4}{4m_{\rm e}^2}} du_x$$

$$= \frac{3\omega_{\rm pe}^2}{4V_{\rm Fe}^3} \int_{-V_{\rm Fe}}^{V_{V\,e}} \frac{V_{\rm Fe}^2 - u_x^2}{(\omega - ku_x)^2 - \frac{\hbar^2 k^4}{4m_{\rm e}^2}} du_x. \tag{2.18}$$

Performing the integration over velocity space, from (2.18) we have

$$\chi_{\rm e} = \frac{3\omega_{\rm pe}^2}{4k^2 V_{\rm Fe}^2} \left\{ 2 - \frac{m_{\rm e}}{\hbar k V_{\rm Fe}} \left[V_{\rm Fe}^2 - \left(\frac{\omega}{k} + \frac{\hbar k}{2m_{\rm e}}\right)^2 \right] \log \left| \frac{\frac{\omega}{k} - V_{\rm Fe} + \frac{\hbar k}{2m_{\rm e}}}{\frac{\omega}{k} + V_{\rm Fe} + \frac{\hbar k}{2m_{\rm e}}} \right| \right.$$

$$\left. + \frac{m_{\rm e}}{\hbar k V_{\rm Fe}} \left[V_{\rm Fe}^2 - \left(\frac{\omega}{k} - \frac{\hbar k}{2m_{\rm e}}\right)^2 \right] \log \left| \frac{\frac{\omega}{k} - V_{\rm Fe} - \frac{\hbar k}{2m_{\rm e}}}{\frac{\omega}{k} + V_{\rm Fe} - \frac{\hbar k}{2m_{\rm e}}} \right| \right\}. \tag{2.19}$$

In the derivation of (2.19), we have assumed that the waves are only weakly damped, so that when integrating over poles, only the principal parts of the integrals are kept. In the limit $\hbar k/m_{\rm e} \to 0$, from (2.19) we have

$$\chi_{\rm e} = \frac{3\omega_{\rm pe}^2}{k^2 V_{\rm Fe}^2} \left(1 - \frac{\omega}{2kV_{\rm Fe}} \log \left| \frac{\omega + kV_{\rm Fe}}{\omega - kV_{\rm Fe}} \right| \right), \tag{2.20}$$

where it holds that ω is real and $\omega/k > V_{\rm Fe}$. Hence in this 'semi-classical' limit, we do not have Landau damping. (We call (2.20) 'semi-classical' because it can be derived from the Vlasov equation for electrons using the flat-topped background electron distribution function given by (2.15).)

3. Electron oscillations

We here consider high-frequency ($\omega \gg \omega_{\rm pi}$) oscillations so that $\chi_i \ll 1$ in (2.6). Then, expanding (2.19) for small wavenumbers up to terms containing k^4, we obtain from (2.10) the dispersion relation

$$\omega^2 = \omega_{\rm pe}^2 + \frac{3}{5} k^2 V_{\rm Fe}^2 + (1+\alpha) \frac{\hbar^2 k^4}{4m_{\rm e}^2}, \tag{3.1}$$

where $\alpha = (48/175) m_{\rm e}^2 V_{\rm Fe}^4 / \hbar^2 \omega_{\rm pe}^2 \approx 2.000 (n_0 a_0^3)^{1/3}$ and $a_0 = \hbar^2/m_{\rm e}e^2 \approx 53 \times 10^{-10}$ cm is the Bohr radius. For a typical metal such as gold, which has a free-electron number density of $n_0 = 5.9 \times 10^{22}$ cm^{-3}, we would have $\alpha \approx 0.4$. For the free-electron density in semiconductors, which is many orders of magnitude less than in metals, α is much smaller and can safely be dropped compared with unity. However, for electron plasma oscillations in dense matters, α could be larger than unity. It should be noted that the term proportional to α in (3.1) was not discussed by Bohm and Pines (1953) and others but was, however, obtained and discussed by Ferrel (1957) in his study of collective electron oscillations in metals (see (10) in his paper, where, in his notation, it should be $(\Delta v^2/v_0^2)^2 = 12/175$).

It is interesting to note that (2.19) *may admit* Landau damping above a certain critical wavenumber, $k > k_{cr}$ and corresponding frequency $\omega > \omega_{cr}$. This occurs if the denominator in the integral of (2.18) vanishes within the integration limits

https://doi.org/10.1017/S0022377809990316 Published online by Cambridge University Press

$u_x = \pm V_{\rm Fe}$. For the critical wavenumber and frequency, we have

$$\omega = \omega_{cr} = k_{cr} V_{\rm Fe} + \frac{\hbar k_{cr}^2}{2} m_{\rm e}. \tag{3.2}$$

Inserting this expression into (2.19) we note that the term involving the logarithm on the second line of (2.19) vanishes, and we obtain the critical wavenumber $k = k_{cr}$ from

$$1 + \frac{3\omega_{\rm pe}^2}{4k_{cr}^2 V_{\rm Fe}^2}\left[2 - \left(2 + \frac{\hbar k_{cr}}{m_{\rm e} V_{\rm Fe}}\right)\log\left(1 + \frac{2m_{\rm e} V_{\rm Fe}}{\hbar k_{cr}}\right)\right] = 0. \tag{3.3}$$

A careful examination of the dispersion relation for $k > k_{cr}$, should involve Landau contours to correctly take into account Landau damping. Here we are interested in low- and high-frequency waves in the weakly damped regime and have postponed the investigation of Landau damping of the system to future studies.

4. Ion oscillations

In a quantum plasma system composed of mobile ions and inertialess electrons, we have the possibility of low-phase-speed (in comparison with the Fermi electron thermal speed) ion-acoustic-like oscillations. For low-frequency ($\omega \ll kV_{\rm Fe}$) waves, from (2.19) we have

$$\chi_{\rm e} = \frac{3\omega_{\rm pe}^2}{2k^2 V_{\rm Fe}^2}\left[1 - \frac{m_{\rm e}}{\hbar k V_{Ve}}\left(V_{\rm Fe}^2 - \frac{\hbar^2 k^2}{4m_{\rm e}^2}\right)\log\left|\frac{V_{\rm Fe} - \frac{\hbar k}{2m_{\rm e}}}{V_{\rm Fe} + \frac{\hbar k}{2m_{\rm e}}}\right|\right]. \tag{4.1}$$

For small wavenumbers $\hbar k \ll m_{\rm e} V_{\rm Fe}$, we have the approximate electron susceptibility, up to terms containing factors of k^4,

$$\chi_{\rm e} \approx \frac{3\omega_{\rm pe}^2}{k^2 V_{\rm Fe}^2 + \hbar k^4/12m_{\rm e}^2}. \tag{4.2}$$

Using the dispersion relation

$$\varepsilon(\omega, k) = 1 + \chi_{\rm e} + \chi_i = 0, \tag{4.3}$$

we employ (2.6) to obtain the frequency of ion acoustic waves as

$$\omega = \frac{\omega_{\rm pi}}{(1 + \chi_{\rm e})^{1/2}}, \tag{4.4}$$

with $\chi_{\rm e}$ given by (4.1) or (4.2). For $\chi_{\rm e}$ given by the approximate expression (4.2), we have

$$\omega = \frac{\omega_{\rm pi}(k^2 V_{\rm Fe}^2 + \hbar^2 k^4/12m_{\rm e}^2)^{1/2}}{(3\omega_{\rm pe}^2 + k^2 V_{\rm Fe}^2 + \hbar^2 k^4/12m_{\rm e}^2)^{1/2}} = \frac{kC_s(1 + \hbar^2 k^2/12m_{\rm e}^2 V_{\rm Fe}^2)^{1/2}}{(1 + k^2 V_{\rm Fe}^2/3\omega_{\rm pe}^2 + \hbar^2 k^4/36m_{\rm e}^2\omega_{\rm pe}^2)^{1/2}}, \tag{4.5}$$

where $C_s = \sqrt{m_{\rm e} V_{\rm Fe}^2/3m_i}$ is the Fermi ion acoustic speed. We note that $\omega \to \omega_{\rm pi}$ as $k \to \infty$.

5. Density regimes of the system

We note that there is a critical density parameter in the system. When the interparticle distance is smaller than the Bohr radius, then the quantum statistical pressure dominates the wave dynamics, while in the opposite case, the quantum

https://doi.org/10.1017/S0022377809990316 Published online by Cambridge University Press

tunnelling effects become important when the wavelength is comparable to the inter-particle distance. This can be seen by normalizing the system such that $\omega/\omega_{\rm pe} = \Omega$ and $kV_{\rm Fe}/\omega_{\rm pe} = K$. Then, (2.19) takes the form

$$\chi_{\rm e} = \frac{3}{4K^2}\left\{2 - \frac{\beta}{K}\left[1 - \left(\frac{\Omega}{K} + \frac{K}{2\beta}\right)^2\right]\log\left|\frac{\frac{\Omega}{K} - 1 + \frac{K}{2\beta}}{\frac{\Omega}{K} + 1 + \frac{K}{2\beta}}\right| + \frac{\beta}{K}\left[1 - \left(\frac{\Omega}{K} - \frac{K}{2\beta}\right)^2\right]\log\left|\frac{\frac{\Omega}{K} - 1 - \frac{K}{2\beta}}{\frac{\Omega}{K} + 1 - \frac{K}{2\beta}}\right|\right\}, \tag{5.1}$$

where

$$\beta = \frac{m_{\rm e}V_{\rm Fe}^2}{\hbar\omega_{\rm pe}} = 3^{2/3}\pi^{5/6}(a_0^3 n_0)^{1/6}. \tag{5.2}$$

In the scaled variables, (2.20) and (3.1) take the forms

$$\chi_{\rm e} = \frac{3}{K^2}\left(1 - \frac{\Omega}{2K}\log\left|\frac{\Omega + K}{\Omega - K}\right|\right) \tag{5.3}$$

and

$$\Omega^2 = 1 + \frac{3}{5}K^2 + \left(\frac{1}{\beta^2} + \frac{48}{175}\right)\frac{K^4}{4}, \tag{5.4}$$

respectively. We note that the limit $\hbar k/m_{\rm e} \to 0$ to obtain (2.20) from (2.19) corresponds to $\beta \to \infty$ to obtain (5.3) from (5.1). For $\beta \gg 1$, the quantum statistical pressure dominates, while for $\beta \ll 1$, the quantum tunnelling effects dominate. Considering the value of β for different physical systems, we note that $\beta = 0.1$ corresponds to relatively low-density degenerate plasma such as in semiconductors, while $\beta = 1$ corresponds to typical free-electron densities in metals. The high-density case $\beta = 10$ corresponds to high-density matter which may be obtained in laser compression schemes or which exist in white dwarf stars. Even though we have formally considered the semi-classical limit $\beta \to \infty$, it should be kept in mind that an upper limit for the validity of our theory is when the electron density becomes high enough so that the Fermi speed $V_{\rm Fe}$ becomes comparable to the speed of light. In this limit, the inter-particle distance $n^{-1/3}$ approaches the Compton length $\lambda_C = 2\pi\hbar/m_{\rm e}c \approx 2.4 \times 10^{-12}$, and we have an electron number density of the order 10^{35} m^{-3}, corresponding to $\beta \approx 27$. For larger values of β, the equilibrium equation of state for the electrons (Chandrasekhar 1935) changes from $P = (2/5)\mathscr{E}_F n_0 (n_{\rm e}/n_0)^{5/3}$ to $P = (3/\pi)^{1/3}(4\pi ch/8)n_{\rm e}^{4/3}$. For this case, we need to include relativistic effects in the electron susceptibility.

In the normalized variables, the condition (3.3) for the critical wavenumber for the limit between undamped and Landau-damped high-frequency waves is given by

$$1 + \frac{3}{4K_{cr}^2}\left[2 - \left(2 + \frac{K_{cr}}{\beta}\right)\log\left(1 + \frac{2\beta}{K_{cr}}\right)\right] = 0, \tag{5.5}$$

and the normalized critical frequency is obtained from (3.2) as

$$\Omega_{cr} = K_{cr} + K_{cr}^2/2\beta, \tag{5.6}$$

where $K_{cr} = k_{cr}V_{\rm Fe}/\omega_{\rm pe}$ and $\Omega_{cr} = \omega_{cr}/\omega_{\rm pe}$.

https://doi.org/10.1017/S0022377809990316 Published online by Cambridge University Press

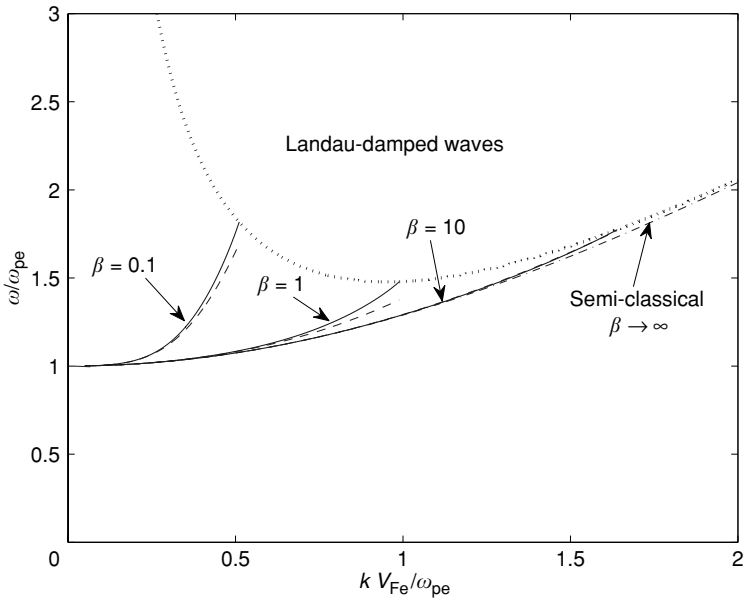

Figure 1. Dispersion curves (ω versus k) for different values of $\beta = m_e V_{Fe}^2/\hbar\omega_{pe}$. The solid curves show solutions of (2.10) using the exact susceptibility (2.19); the dashed curves show the expanded solution (3.1); and the dash-dotted curve shows shows the solutions of (2.10) using the 'semi-classical' electron susceptibility (2.20). The dotted curve indicates the border between undamped waves and Landau-damped waves, given by (3.2) and (3.3) (or (5.5) and (5.6)).

Finally, for the low-frequency case, the electron susceptibilities (4.1) is in the normalized variables given by

$$\chi_e = \frac{3}{2K^2}\left[1 - \frac{\beta}{K}\left(1 - \frac{K^2}{4\beta^2}\right)\log\left|\frac{1-\frac{K}{2\beta}}{1+\frac{K}{2\beta}}\right|\right], \tag{5.7}$$

and the expression for small wavenumbers (4.2) is given by

$$\chi_e \approx \frac{3}{K^2 + \hbar K^4/12\beta^2}. \tag{5.8}$$

6. Numerical results

In Figs 1 and 2, we show dispersion curves for the high-frequency ($\omega \gg \omega_{pi}$) waves for different values of β, obtained from the solutions of the dispersion relation (2.10), by using the electron susceptibility (2.19), as well as the expansion (3.1) and the limiting semi-classical case (2.20). We have also indicated the border between undamped and Landau-damped waves, obtained from (3.2) and (3.3). We note that the dispersion curve for the semi-classical case in Fig. 1 always lies in the undamped regime, below the border between undamped and Landau-damped waves. For the undamped waves, expansion (3.1) approximates the exact dispersion relation within a few per cent and can therefore be used instead of (2.19) for most cases. This holds especially for small wavenumbers, as can be seen in the close-up in Fig. 2.

https://doi.org/10.1017/S0022377809990316 Published online by Cambridge University Press

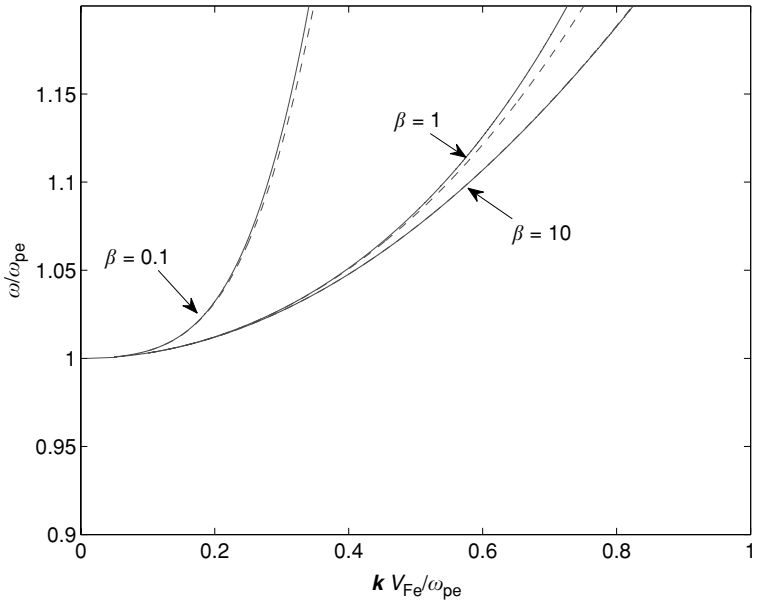

Figure 2. Close-up of the dispersion curves in Fig. 1.

The dispersion curves for the low-frequency ion-acoustic oscillations are plotted in Fig. 3, where we have depicted the ω in (4.4) for χ_e, given by the exact expression (4.1) and the approximate expansion (4.2), and for different values of β. We note that the dispersion curves show agreement at small wavenumbers but deviate significantly for larger wavenumbers in the case $\beta = 0.1$, while the agreement is better for $\beta = 1$ and excellent for $\beta = 10$. It should be kept in mind that when $\hbar k \sim m_e V_{Fe}$, the wavelength of the oscillations is comparable to the inter-particle distance, and there will be corrections because of the discrete nature of the ion background. Thus, the theory is not valid for oscillations with $\hbar k \gg m_e V_{Fe}$.

7. Conclusions

In this paper, we have studied the dispersion properties of electrostatic oscillations in quantum plasmas for different parameters ranging from semiconductor plasmas to typical metallic electron densities and densities corresponding to compressed matter and dense astrophysical objects. We have derived a simplified expansion that accurately approximates the exact dispersion relation for small wavenumbers. The possibility of Landau damping owing to quantum tunnelling effects at large wavenumbers has also been discussed, and conditions for Landau damping have been derived. The present results should be useful in understanding the salient features of electrostatic plasma oscillations in dense plasmas with degenerate electrons. The latter are encountered in metals, in highly compressed intense laser–solid density plasma experiments and in compact astrophysical objects (e.g. interior of white dwarf stars).

https://doi.org/10.1017/S0022377809990316 Published online by Cambridge University Press

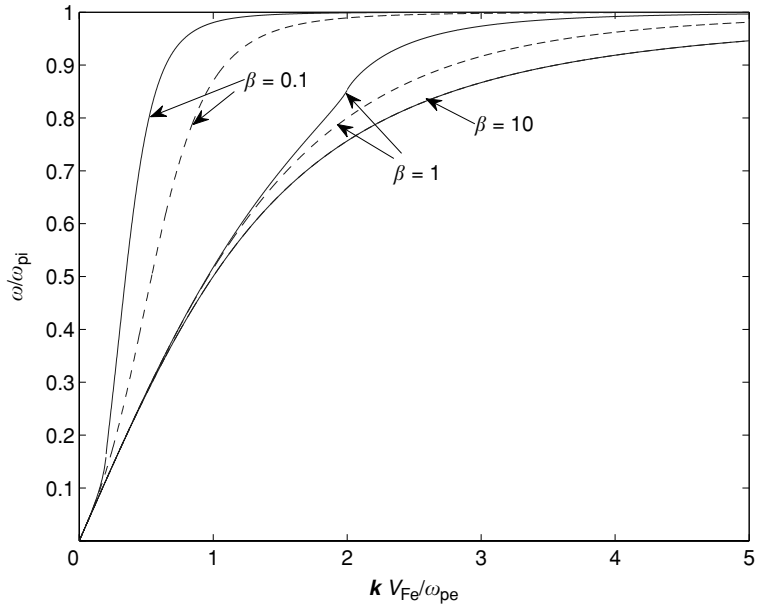

Figure 3. Dispersion curves (ω versus k) for the low-frequency ion oscillations, for different values of $\beta = m_e V_{Fe}^2/\hbar\omega_{pe}$. The solid curves show the wave frequency given by (4.4) using the low-frequency electron susceptibility (4.1), while the dashed curves use the approximate electron susceptibility (4.2). For $\beta = 10$ the solid and dashed curves are indistinguishable.

Acknowledgements

This work was supported by the Deutsche Forschungsgemeinschaft through project SH21/3-1 of Research Unit 1048 and by the Swedish Research Council (VR).

References

Azechi, H., Jitsuno, T., Kanabe, T., Katayama, M., Mima, K., Miyanaga, N., Nakai, M., Nakai, S., Nakaishi, H., Nakatsuka, M. et al. 1991 High-density compression experiments at ILE, Osaka. *Laser Part. Beams* **9**, 193–207.

Azechi, H., and the FIREX Project 2006 Present status of the FIREX programme for the demonstration of ignition and burn. *Plasma Phys. Control. Fusion* **48**, B267–B275.

Bohm, D. 1952. A suggested interpretation of the quantum theory in terms of 'hidden' variables. I. *Phys. Rev.* **85**, 166–179.

Bohm, D. and Pines, D. 1953 A collective description of electron interactions. III. Coulomb interactions in a degenerate gas. *Phys. Rev.* **92**, 609–625.

Bonitz, M., Semkat D., Filinov A., et al. 2003 Theory and simulation of strong correlations in quantum coulomb systems. *J. Phys. A: Math. Gen.* **36**, 5921–5930.

Chandrasekhar, S. 1935 The highly collapsed configurations of a stellar mass (second paper). *MNRAS* **95**, 207–225.

Crouseilles, N., Hervieux P.-A. and Manfredi, G. 2008 Quantum hydrodynamic models for nonlinear electron dynamics in thin metal films. *Phys. Rev.* B **78,** 155412.

Ferrel, R. A. 1957 Characteristic energy loss of electrons passing through metal foils. II. Dispersion relation and short wavelength cutoff for plasma oscillations. *Phys. Rev.* **107**, 450–462.

Glenzer, S. H., Landen, O. L., Neumayer, P., Lee, R. W., Widmann, K., Pollaine, S. W., Wallace, R. J., Gregori, G., Höll, A., Bomath, T. et al. 2007 Observations of plasmons in warm dense matter *Phys. Rev. Lett.* **98**, 065002.

Klimontovich, Y. and Silin, V. P. 1961 The spectra of systems of interacting particles. In Plasma Physics (ed. J. E. Drummond) New York: McGraw-Hill, ch. 2, pp. 35–87.

Klimontovich, Y. L. and Silin, V. P. 1952 *Doklady Akad. Nauk S.S.S.R.* **82**, 361. Also published in *J. Exp. Teoret. Fis.* **23**, 151.

Kritcher, A. L., Neumayer, P., Castor, J., Döppner, T., Falcone, R. W., Landen, O. L., Lee, H. J., Morse, E. C., Ng, A., Pollaine, S. et al. 2008 Ultrafast X-ray Thomson scattering of shock-compressed matter. *Science* **322**, 69–71.

Lee, H. J., Neumayer, P., Castor, J., Döppner, T., Falcone, R. W., Fortmann, C., Hammel, B. A., Kritcher, A. L., Landen, O. L., Lee, R. W. et al. 2009 X-Ray Thomson-scattering measurements of density and temperature in shock-compressed beryllium. *Phys. Rev. Lett.* **102**, 115001.

Lindl, J. 1995 Development of the indirect-drive approach to inertial confinement fusion and the target physics basis for ignition and gain. *Phys. Plasmas* **2**, 3933.

Manfredi, G. 2005 How to model quantum plasmas. *Fields Inst. Comm.* **46**, 263–287.

Mendonça, J. T., Ribeiro, E. and Shukla, P. K. 2008 Wave kinetic description of quantum electron-positron plasmas. *J. Plasma Phys.* **74**, 91–94.

Pines, D. 1961 I. Quantum plasma physics: classical and quantum plasmas. *J. Nucl. Energy: Part C: Plasma Phys.* **2,** 5–17.

Serbeto A., Mendonça, J. T., Tsui, K. H. and Bonifacio, R. 2008 Quantum wave kinetics of high-gain free-electron lasers. *Phys. Plasmas* **15**, 013110.

Shaikh, D. and Shukla, P. K. 2007 Fluid turbulence in quantum plasmas. *Phys. Rev. Lett.* **99**, 125002.

Shukla, P. K. 2009 A new spin on quantum plasmas. *Nature Phys.* **5**, 92–93.

Shukla, P. K. and Eliasson, B. 2006 Formation and dynamics of dark solitons and vortices in quantum electron plasmas. *Phys. Rev. Lett.* **96**, 245001.

Son, S. and Fisch, N. J. 2005 Current-drive efficiency in a degenerate plasma. *Phys. Rev. Lett.* **95,** 225002.

Tabak, M., Hammer, J., Glinsky, M. E., Kruer, W. L., Wilks, S. C., Woodworth, J., Campbell, E. M., Perry, M. D. et al. 1994 Ignition and high gain with ultrapowerful lasers. *Phys. Plasmas* **1**, 1626–1634.

Tabak, M., Clark, D. S., Hatchett, S. P., Key, M. H., Lasinski, B. F., Snavley, R. A., Wilks, S. C., Town, R. P. J., Stephens, R., Kampbell, E. M. et al. 2005 Review of progress in fast ignition. *Phys. Plasmas* **12,** 057305.

Watanabe, H. 1956 Experimental evidence for the collective nature of the characteristic energy loss of electrons in solids –studies on the dispersion relation of plasma frequency. *J. Phys. Soc. Jpn* **11**, 112–119.